Impact of Sorghum Racial Structure and Diversity on Genomic Prediction of Grain Yield Components

Sirjan Sapkota,* Richard Boyles, Elizabeth Cooper, Zachary Brenton, Matthew Myers, and Stephen Kresovich

Affiliations: S. Sapkota, Z. Brenton, M. Myers and S. Kresovich, Advanced Plant Technology Program, Clemson University, Clemson, SC 29634; S. Sapkota, R. Boyles, and S. Kresovich, Department of Plant and Environmental Sciences, Clemson University, Clemson SC 29634; R. Boyles, Pee Dee Research and Education Center, Clemson University, Florence, SC 29506; E. Cooper, Department of Bioinformatics and Genomics, University of North Carolina at Charlotte, Charlotte, NC 28223. Received _____. *Corresponding author (ssapkot@g.clemson.edu).

Abbreviations: AR, across race; BL, terminal branch length; BLUE, best linear unbiased estimator; CV, cross validation; DTA, days to anthesis; FLH, flag leaf height; GEBV, genomic estimated breeding values; GN, grain number; GW, grain weight; GY, grain yield; LD, linkage disequilibrium; MAF, minor allele frequency; PCA, principal component analysis; PH, plant height; PL, panicle length; GBLUP: genomic best linear unbiased prediction; *r*: prediction accuracy; SRT, single race training; WR, within race.

ABSTRACT

Population structure is an important factor that affects the accuracy of estimated breeding values. Natural sorghum populations exhibit population structure resulting from genetic and morphological differentiation due to evolutionary divergence. To study the impact of sorghum racial structure and diversity in genomic prediction, we conducted two cross validation (CV) experiments: CV1; proportional sampling from races, and 2) CV2; sampling from across race (AR) or within race (WR). A diversity panel with 389 individuals with 224,007 single nucleotide polymorphism markers were used for genomic prediction. The prediction accuracy (*r*) for CV1 ranged from 0.52 to 0.69, but *r* declined by 39% and 54% on average for WR and AR methods, respectively. Grain weight was consistently the best predicted trait across all methods except AR. Expectedly, the contribution of race towards CV1 accuracy ranged from a third to a half for grain and panicle traits whereas race was a bad predictor of plant height. Genomic heritabilities were positively correlated (0.63) with mean *r*, and within-subpopulation variance accounted for about 80% of total genetic variance. The difference between average *r* for WR and AR was greater in durra and caudatum, small in kafir, and nonexistent in guinea and mixed. Furthermore, we observed higher prevalence of minor alleles among guinea and mixed subgroups highlighting contribution of allelic diversity towards prediction accuracy. Genomic prediction in sorghum will benefit from utilization of inter-racial diversity and we emphasize the need for further investigations into the role of racial structure in genomic prediction.

INTRODUCTION

Cultivated crops have undergone genetic bottlenecks as a result of domestication and artificial selection. Genetic diversity in modern crops is further reduced by current plant breeding practices because most of the cultivars are derived from genetically-related varieties that represent a very small fraction of the global diversity of plant germplasm for any species (McCouch, et al., 2013). Effective utilization of genetic diversity to increase resilience and crop yield potential will remain a key aspect to meet the projected food demands in the next few decades and reduce vulnerability to biotic and abiotic stresses,.

Sorghum is an important cereal crop grown and consumed as a staple by over half a billion people in the semi-arid tropics. The earliest known record of sorghum seeds are the charred remains from 8000 years before present found at Nabta Playa near the Egyptian-Sudanese border during archeological excavations (Wendorf, et al., 1992). After early domestication likely near the Sahel region of sub-Saharan Africa, further migration and adaptation of early sorghum domesticates occurred across Africa and Asia. Those demographic events led to the evolution of morphologically and geographically diverse groups that are classified into five major races and 10 intermediate races of sorghum (Harlan and de Wet, 1972, Harlan and Stemler, 1976). This phenotype-based classification of sorghum races has been supported by genetic evidences in a global diversity panel (Brown, et al., 2011). Furthermore, the linkage disequilibrium (LD) in sorghum has shown presence of strong genetic bottleneck and patterns of disruptive selection across the sorghum genome as a result of domestication, adaptation, and diversifying selection (Mace, et al., 2013, Morris, et al., 2013, Wang, et al., 2013).

61 The sorghum conversion program (SCP) was initiated by the United States Department of
62 Agriculture (USDA) in cooperation with Texas A&M University to introduce novel genetic
63 variation from exotic tropical germplasm by converting selected tropical genotypes to temperate
64 adapted, photoperiod-insensitive lines with short stature (Stephens et al. 1967). This ongoing
65 initiative has been the staple source of germplasm for several public and private breeding
66 programs in temperate regions. However, the conversion of tropical lines through repeated
67 backcrossing is an expensive and labor-intensive process. Therefore, only 1000-1500 tropical
68 lines have been converted, and these converted lines represent a limited fraction of USDA and
69 worldwide collection of sorghum germplasm (Bob Klein, personal communication). Recent
70 advances in genomic and computational capabilities present opportunities for identifying
71 effective strategies for introducing and screening of germplasm for novel genetic variation,
72 which can benefit breeders by making selection of prebreeding germplasm more accurate and
73 meaningful.

74 Genomic prediction (also known as genomic selection or genome-wide selection) is a
75 method to simultaneously estimate the effects of all genetic markers and use those marker effects
76 to estimate breeding values (Meuwissen et al. 2001; Bernardo and Yu 2007). The marker effects
77 are estimated using both genotypic and phenotypic data from a training population, which can
78 then be used to predict genomic estimated breeding value (GEBV) using only the genotypic
79 information in a testing population. The accuracy of prediction is measured as the correlation
80 between GEBVs and true genetic values, often represented by observed phenotypic values.
81 Genomic prediction is usually applied in breeding populations where the training and testing
82 population have a shared pedigree, but its application can be extended to screening and selection
83 for pre-breeding or population improvement (Yu et al. 2016; Gaynor et al. 2017). Every year, an

84 increasingly larger number of association studies are conducted for allele mining by breeding
85 and genetics programs across the world. Large-volume phenotypic datasets generated from these
86 studies can be applied in the investigation and application of genomic prediction models across
87 ranges of crops and traits. These resources can then be utilized in careful strategies to tap into the
88 large number of gene bank accessions by screening for useful genetic variation with potential to
89 enhance genetic gain (Yu et al. 2016).

90 The implementation of genomic prediction in a diverse and stratified population,
91 however, requires careful consideration of the genomic relationship and population structure
92 (Jannink et al. 2010; Habier et al. 2007). Population structure has been shown to affect the
93 accuracy of genomic prediction in stratified populations across several crop species (Guo, et al.,
94 2014, Ly, et al., 2013, Norman, et al., 2018). Population structure analysis can be done using
95 non-model based approaches like principal component analysis (Patterson et al. 2006; Price et al.
96 2006) or model based clustering approaches like ADMIXTURE (Alexander et al. 2009).
97 Incorporating population structure estimates into both association and prediction studies has
98 proven useful, but the methods for including population structure in the model can vary. While
99 the inclusion of population structure as a covariate has been successfully applied in mixed
100 models for association studies, the use of population structure as fixed effects in genomic best
101 linear unbiased prediction (GBLUP) models would be concerning because they already enter into
102 the model as random effects (de los Campos and Sorensen, 2014, Janss, et al., 2012, Price, et al.,
103 2010). One approach to account for population structure in genomic prediction is designing a
104 cross validation scheme that ensures equal representation of each subpopulation in training and
105 validation sets (Albrecht, et al., 2011, Guo, et al., 2014). Alternatively, in order to avoid biased
106 estimation due to the presence of genetic structure and familial relatedness, prediction analysis

107 can be performed by partitioning the genomic variability into within and across group
108 components (Guo, et al., 2014, Norman, et al., 2018, Technow, et al., 2012). Because of distinct
109 racial structure in sorghum, an approach to account for contribution of racial structure in
110 prediction accuracy by decomposing variance-covariance components into expectations due to
111 race and covariance from individuals within a race could be beneficial.

112 A recent simulation study has highlighted the advantages of genomics-assisted recurrent
113 selection over phenotypic recurrent selection in a nascent and small sorghum breeding program,
114 emphasizing the need for further investigations on genomic selection in sorghum (Muleta, et al.,
115 2019). Since inter-racial diversity is important for heterotic gain, application of genomic
116 prediction in sorghum breeding will benefit from investigations into the effect of racial structure
117 on prediction accuracy. While the effect of population structure in genomic prediction has been
118 extensively studied in major cereal crops, the distinctive evolutionary history and racial structure
119 of sorghum merits the need for investigation into the effect of sorghum racial structure in
120 genomic prediction (Guo, et al., 2014, Isidro, et al., 2015, Norman, et al., 2018). A previous
121 study examined the effect of genetic relatedness on genomic prediction of pedigreed male lines
122 in a sorghum breeding program, however, there has been no studies on the role of sorghum racial
123 structure in genomic prediction (Hunt, et al., 2018). The objectives of our study were to estimate
124 genetic structure and diversity among sorghum races and implement genomic prediction for plant
125 architecture and grain yield traits to examine the effect of racial structure on prediction accuracy
126 using a grain diversity panel.

MATERIALS AND METHODS

Plant materials, field design, and phenotyping

The sorghum diversity panel used in this study consisted of 389 diverse sorghum accessions, including 332 accessions from the United States sorghum association panel (SAP) developed by Casa, et al. (2008). Additional accessions were included for diversity and elite grain characteristics (Boyles, et al., 2016). The population was planted in randomized complete block design with two replications in 2013, 2014, and 2017 field seasons at the Clemson University Pee Dee Research and Education Center in Florence, South Carolina. The accessions were assigned to blocks within the replication based on height, maturity, and photoperiod sensitivity. Each plot was two 6.1 m rows spaced 0.726 m apart with a targeted planting density of 130,000 plants ha^{-1} assuming 75% plant establishment rate. In 2017, an average plant density of ~62,350 plants ha^{-1} was calculated based on plant stand count and row length at 24 days after planting (DAP). Fields were irrigated when plants showed signs of stress in order to avoid confounding effects of maturity and varying degree of drought tolerance in the population on yield. The details on agronomic practices for 2013 and 2014 can be found in Boyles, et al. (2016). In 2017, a lay-by of 93 Kg ha^{-1} N was applied at 35 DAP in addition to variable rate of fertilizer (N, P, K) applications before planting. Preemergence and postemergence herbicide applications in 2017 were consistent with 2013 and 2014. A single application of 0.5 L ha^{-1} of Sivanto™ Prime (Bayer CropScience) was administered at 60 DAP to control sugarcane aphid population.

Three consecutive plants from the odd row of each plot was selected for phenotyping in order to prevent biases due to row effect. We also avoided plants from beginning and end of the row to account for border effect. The detail procedures for phenotyping of agronomic and grain phenotypes has previously been described in Boyles et. al. (2016; 2017) . Days to anthesis

150 (DTA) for each plot was measured as the number of days from planting to when 50% of the
151 plants in the plot were at mid-bloom. Plant height (PH) was measured from ground to the apex of
152 the primary panicle at physiological maturity. Flag leaf height (FLH), panicle length (PL), and
153 terminal branch length (BL) of each plant harvested in 2017 were measured. Flag leaf height was
154 measured as the height from ground to the flag leaf of the plant. Panicle length was measured as
155 length of primary panicle from the terminal branch to the apex of the panicle, and BL was
156 measured as length of the two terminal primary branches, respectively. A more detailed
157 description of these inflorescence architecture traits can be found in Brown, et al. (2006). Grain
158 yield components were phenotyped from primary panicle of three consecutive plants harvested at
159 physiological maturity as previously mentioned. Panicles were air dried to a constant moisture
160 (10-12%) before threshing. Threshed seed were processed through seed counters (Old Mill
161 Model 900-2) to measure grain number per primary panicle (GN). Grain yield per primary
162 panicle (GY) in grams (g) was measured with a Discovery series scale (Ohaus). Subsequently,
163 thousand grain weight (GW) was calculated from GY and GN; GW (g) = (GY/GN) × 1000.

164 **Phenotypic analysis**

165 R statistical software was used for phenotypic analysis (R Development Core Team, 2016).
166 Simple mean of phenotypic values were calculate for each replication with the years. The
167 phenotypic means of the traits were fitted into a linear mixed model analysis using lme4 package
168 in R (Bates, et al., 2015). We fit the following mixed model equation:

169 $$y_{ijk} = \mu + G_i + E_j + G_iE_j + R_k(E_j) + e_{ijk}, \qquad (1)$$

170 where y_{ijk} is the phenotypic value for genotype i, year j, and replication k within the year
171 j; μ is the population mean; G_i is the fixed effects of ith genotype; E_j, GE_{ij}, $R_k(E_j)$ are random
172 effects of year, genotype × year, and replication within the year, respectively; and e_{ijk} is the

173 random effect of residuals, with $e \sim N(0, \sigma_e^2)$. Since phenotypes for PL, BL and FLH were only
174 available from the year 2017, the model was fit with just the random effect of replications within
175 the year and fixed effect of genotypes. Best linear unbiased estimates (BLUEs) for the traits were
176 calculated from the fixed effect of the genotypes. Correlation plots and histograms for the
177 estimated phenotypic means were generated using the *pairs.panels* function within the R
178 package Psych (Revelle, 2011).

179 **Genotyping**

180 Genetic characterization of the diversity panel was done using genotyping-by-sequencing (GBS)
181 as previously described in Morris, et al. (2013). Sequenced reads were aligned to the sorghum
182 reference assembly (BTx623 v3.1, www.phytozome.net) using burrow-wheelers aligner (Li and
183 Durbin 2010). SNP calling, imputation and filtering were done using the TASSEL 5.0 pipeline
184 (Glaubitz, et al., 2014). A total of 515,318 SNPs was called and subsequently imputed using the
185 *FILLINFindHaplotypesPlugin* and *FILLINImputationPlugin* in TASSEL. FILLIN (Fast, Inbred
186 Line Library ImputatioN) imputes missing genotypes by: (1) haplotype generation using inbred
187 segments that share identity by state, and (2) imputation of resulting haplotypes back onto the
188 target samples (Swarts, et al., 2014). SNP sites were filtered to remove sites with a minor allele
189 frequency (MAF) < 0.01, and sites present in at least 90% of the individuals were retained. A
190 final SNP matrix with a total of 224,007 SNPs was created and used for subsequent genomic
191 analysis and predictions. In the final SNP matrix, all genotypes had less than 10% missing sites.
192 The final SNP genotype matrix was further filtered to retain SNPs with MAF > 0.05 for
193 estimation of the decay of linkage disequilibrium (LD).

194 **Population structure and genetic diversity**

195 The final SNP matrix was used to first identify the optimum number of clusters based on cross
196 validation of error, then used to calculate the ancestry coefficients using ADMIXTURE
197 (Alexander, et al., 2009). Admixture ancestry coefficients (Q matrix) were estimated using the
198 default block relaxation algorithm. We also calculated covariances for the first five principal
199 components (PCs) using the SNP data in TASSEL. A common subset of 35,277 SNPs between
200 the diversity panel and *S. propinquum* from Mace, et al. (2013) was used for neighbor joining
201 tree estimation using the *Cladogram* function in TASSEL. This function first calculates distance
202 between each pair of taxa using modified Euclidean distance (homozygote is 100% similar to
203 itself and heterozygote is 50% similar to itself) and then estimates tree using neighbor joining
204 algorithm (Glaubitz, et al., 2014). The tree was visualized using the web based software
205 Interactive Tree of Life (Letunic and Bork, 2016).

206 Nucleotide diversity (θ_π), Tajima's D, and genetic differentiation (F_{st}) was estimated
207 from the final SNP matrix with the *vcftools* program (Danecek, et al., 2011) using a non-
208 overlapping sliding window of 100 kb. The window size of 100 kb was chosen to avoid sampling
209 error that could arise from variabilities in SNP marker distribution when low coverage
210 sequencing is used for genotyping (Gusnanto, et al., 2014). Minor allele frequency for each SNP
211 site was also calculated using *vcftools*. Linkage disequilibrium was calculated for pairs of alleles
212 using a sliding window of 50 SNPs in TASSEL, and decay of LD with distance was evaluated
213 using non-linear regression *nls* function in R (R Development Core Team, 2016) with a
214 maximum iteration of 100. Expected values of squared allele-frequency correlation (r^2) under
215 drift equilibrium was calculated using the equation from Hill and Weir (1988) as explained in
216 Remington, et al. (2001). Then, average r^2 and average LD half decay distance (bp) were

calculated. Nei's expected heterozygosity was calculated on a per locus basis using the *heterozygosity* function in the R package Pegas (Nei, 1987, Paradis, 2010). Average expected heterozygosity was calculated as mean of heterozygosity across all polymorphic sites.

Genomic prediction and heritability

Statistical model for prediction

Genomic best linear unbiased prediction (GBLUP) model was implemented using *kin.blup* function in R package rrBLUP (Endelman, 2011). In the GBLUP model:

$$y = \mu + g + e, \qquad (2)$$

y is a vector of phenotype BLUEs; μ is the overall mean; **g** is a vector of random effect of genotypes with $g \sim N(0, \boldsymbol{A}\sigma_g^2)$, where σ_g^2 is additive genetic variance and $\boldsymbol{A}$ is the realized additive relationship matrix calculated from $n \times m$ genotype matrix with n number of genotypes and m number of markers using *A.mat* function from rrBLUP package (Endelman and Jannink, 2012); and **e** is a vector of residuals that are identical and independently distributed with $e \sim N(0, \boldsymbol{I}\sigma_e^2)$, where σ_e^2 is the residual variance and $\boldsymbol{I}$ is an identity matrix.

Estimation of genomic heritability

A re-parameterization of GBLUP model as explained in Janss, et al. (2012) was done to evaluate the impacts of population structure on genomic heritability of the traits. The reparameterized model can be written as:

$$y = 1\mu + U\alpha + e, \qquad (3)$$

In the above equation, **U** is an $n \times (n - 1)$ matrix of the eigenvectors obtained from eigenvalue decomposition of additive relationship matrix ($\boldsymbol{A}$) with $\mathbf{U}_i$ the column i ($i = 1, 2, \ldots, n - 1$) of **U** representing the principal component loads; α is an $(n - 1) \times 1$ vector of random effects with normal distribution $N(0, \mathbf{D}\sigma_g^2)$ where **D** is an $(n - 1) \times (n - 1)$ diagonal matrix with

240 each diagonal element representing eigenvalues of ***A*** corresponding to that particular column.
241 The model (3) with principal components as random variables generates the same marker
242 distribution as model (2), and allows for separation of total genetic variance σ_{g}^2 into across-
243 subpopulation genetic variance σ_{gA}^2 due to population structure, and within-subpopulation
244 genetic variance σ_{gW}^2. This partitioning of total genetic variance allowed for estimation of within
245 ($\mathrm{h}_{\mathrm{gA}}^2$) and across-subpopulation ($\mathrm{h}_{\mathrm{gW}}^2$) genomic heritabilities which were calculated as:
246

247 $$\mathrm{h}_{\mathrm{gA}}^2 = \frac{\frac{1}{n}\sum_{i=1}^{d} \alpha_i^2}{\frac{1}{n}\sum_{i=1}^{n} \alpha_i^2 + \sigma_{\mathrm{e}}^2}$$

248 and

249 $$\mathrm{h}_{\mathrm{gW}}^2 = \frac{\frac{1}{n}\sum_{i=d+1}^{n} \alpha_i^2}{\frac{1}{n}\sum_{i=1}^{n} \alpha_i^2 + \sigma_{\mathrm{e}}^2}$$

250 where *d* is largest eigenvectors in the population with *n* individuals used to account for
251 population substructure that result in artifact variation arising due to population admixture. The
252 parameters μ, σ_{gA}^2, σ_{gW}^2, σ_{g}^2, and σ_{e}^2 were estimated by Markov Chain Monte Carlo (MCMC)
253 using a Gibbs sampler as proposed by De Los Campos, et al. (2010) and Janss, et al. (2012) for
254 each trait using phenotypic and genotypic data for all individuals in our panel. A total of 37,000
255 MCMC iterations were run with first 2000 iterations discarded for burn-in. The posterior means
256 for within and across-subpopulation heritabilities were calculated form the estimated variance
257 components.

Cross validation and prediction accuracy

Cross validation using stratified sampling (CV1)

A common cross validation approach using five-folds obtained by stratified sampling was done for CV method 1 (CV1). In stratified sampling, the individuals were proportionally sampled from each sorghum race to form cross-validation folds that have population structure similar to that of the whole population. As illustrated in Figure 1A, individuals within each race were randomly partitioned into five mutually exclusive groups (W_1, W_2, W_3, W_4, and W_5) with similar sample sizes resulting in five proportionally divided datasets (one per race). Then, five subsets (S_1, S_2, S_3, S_4, and S_5) were constructed such that each subset contained one of the partitions from each race (Figure 1A). During cross validation, each subset was treated as a fold, and four of the folds were assigned to the training set and the genetic values were predicted for the remaining fold. This process was repeated until every single fold and individuals were predicted only once, and the predicted genetic values for all individuals were stored. Prediction accuracy was calculated as correlation between predicted genetic values and observed phenotypic values of all individuals in the population for each cross validation run. A similar approach has previously been applied to study the effect of population structure in prediction results (Albrecht, et al., 2011, Guo, et al., 2014). Since all cross-validation folds are proportionally sampled from structured subpopulations, the training and validation sets used in prediction have similar racial structure.

The accuracy from CV1 method was decomposed into covariances resulting from conditional expectations due to racial structure. The decomposition of covariance was calculated as described in Sorensen and Gianola (2007):

$$\mathrm{Cov}(x, y) = \mathrm{E}_{\mathrm{race}}\,[\mathrm{Cov}(x, y|\mathrm{race})] + \mathrm{Cov}_{\mathrm{race}}\,[\mathrm{E}(x|\mathrm{race}), \mathrm{E}(y|\mathrm{race})] \qquad (4)$$

where, x and y are predicted and observed values, respectively; E_{race} is expectation over races of the covariances within race; and Cov_{race} is covariance across races of the expectation within race. A multi-response model with unstructured variances was fitted with scaled values of x and y as response variables, and race as a random variable in the model using the *MCMCglmm* function in the R package MCMCglmm (Hadfield, 2010). A total of 13,000 iterations were done with 3,000 burn-ins, and posterior mean was calculated from a total of 1000 estimates were recorded using a thinning interval of 10.

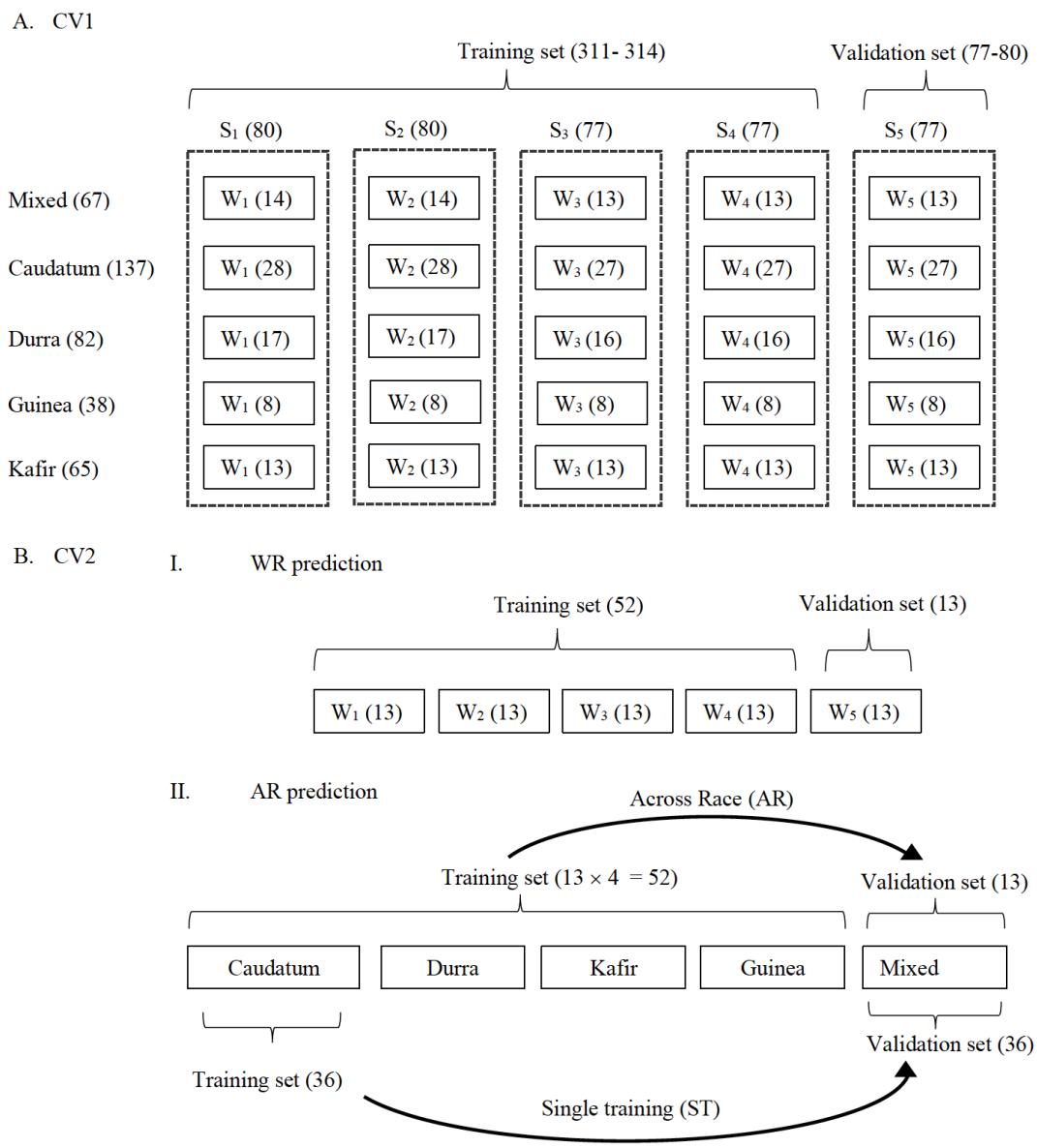

289 **Figure 1**. Examples for cross-validation approaches implemented in the sorghum diversity panel.
290 A) CV1, individuals in each race were proportionally divided into five datasets (W_1,…,W_5) and
291 cross validation fold (S_1,…,S_5) was created as shown by rectangular boxes with broken lines ; B)
292 CV2: within race (WR, I) and across race (AR, II) cross validation method for mixed race. A
293 variation of AR prediction, single race training (SRT), was also implemented where a single race
294 was used for training instead of all four races. In parentheses are the number of individuals used
295 in prediction.

296 **Across and within race cross validations (CV2)**

297 While the CV1 method simulates similar population structure across both training and validation
298 populations, breeding populations are often derived from genetically distinct pedigrees with
299 dissimilar population structure. In order to understand how the GBLUP model for grain yield
300 related traits in sorghum is affected by intrinsic racial structure, we designed a second cross
301 validation experiment, CV2. In this approach, we ran predictions either by dividing individuals
302 from a single race into training and validation folds, or by using individuals from certain race/s
303 as a training population to predict genetic values of individuals from unrelated race/s (Fig 1B).
304 Similar strategies have previously been reported for within and across group genomic prediction
305 for diversity panels in maize and rice (Guo, et al., 2014), and for breeding population in wheat
306 (Norman, et al., 2018).

307 The first CV2 method, within race (WR) prediction, was done by randomly dividing
308 individuals within a single race into five proportional folds (Fig 1B). The five-folds are used for
309 five-fold cross validation, the predicted values for individuals in each fold was stored and
310 subsequently a single *r* was calculated for each cross validation run, as previously described for
311 CV1 method. The five folds in this method are derived from the five mutually exclusive datasets

312 (W_1, W_2, W_3, W_4, and W_5) that were used in CV1 for each race; however, in this method, four of
313 these datasets/folds collectively formed the training set and the remaining dataset/fold was used
314 as validation set. For each run, the predicted values were stored until each fold was predicted
315 once, then a single *r* for calculated as correlation between predicted and observed phenotypic
316 values for the given race.

317 In the second CV2 method, across race (AR) prediction was conducted using four of the
318 races as training population and the fifth race as a validation race (Fig 1B). Unlike in CV1, AR
319 doesn't have a uniform population structure across the folds and the individuals in the training
320 and validation populations are from genetically distinct racial clusters. In order to maintain the
321 same training population size between AR and WR predictions, we sampled proportional amount
322 of individuals from each race to makeup the total cross-validation sample size equal to the sum
323 total of individuals within the validation race. For example as shown in Figure 1B, a total of 13
324 individuals from each of the four races kafir, caudatum, durra, and guinea were sampled as
325 training population ($n = 13 \times 4$) and breeding values were estimated for a random sample of 13
326 individuals from the mixed race. Subsequently, *r* for the mixed race was calculated as correlation
327 for observed phenotypic values and predicted genetic values for those 13 randomly sampled
328 individuals from the mixed race. Similarly, *r* for AR prediction of each race was calculated in
329 similar fashion with a total of 13, 16, 27, and seven individuals sampled from each race for
330 prediction of the races kafir, durra, caudatum, and guinea, respectively. In addition to AR
331 method we also ran a variation of across subpopulation prediction, which we call single race
332 training (SRT) method, where a single fold of 36 individuals sampled from a single race was
333 used as the training population to obtain predicted genetic values of individuals from all other
334 races (Fig 1B). The prediction accuracies for the SRT method were calculated as correlations

335 between predicted and observed values for pairwise combination of training and validation races.
336 The objective of this method was to explore the predictive relationship between any two races
337 for a given trait.
338 A total of 100 random replications were conducted for each cross-validation method, and
339 estimates for mean *r* and standard deviations were calculated. Vectoral graphs used in the
340 analysis of results were created using various plotting functions in R package ggplot2 (Wickham,
341 2016).

342 **RESULTS**

343 **Racial structure**

344 Admixture ancestry coefficients (Q) were used to assign individuals into subpopulations,
345 individuals with coefficients >50% were assigned into that subpopulation. Four of the five
346 subpopulation clusters, thus identified, were broadly congruent with original racial classification
347 of the accessions based on morphological characteristics (Figure 2a, Supplementary Datafile).
348 The remaining accessions contained mixed ancestry based on admixture components, and a large
349 proportion of them belonged to intermediate or mixed races based on original morphological
350 classification (Casa, et al., 2008). For ease, the subpopulation clusters are referred to as
351 corresponding race and "mixed" race represents the cluster of accessions with mixed or
352 intermediate ancestry. Our results from admixture were supported by the principal component
353 and neighbor joining analyses (Figure 2). In the neighbor joining tree, *S. propinquum*, an
354 outgroup individual which is a diploid wild sorghum from southeast Asia, clustered together with
355 accessions from the race guinea suggesting potentially earlier adaptation and divergence of
356 guinea race compared to caudatum, durra, and kafir (Figure 2c).

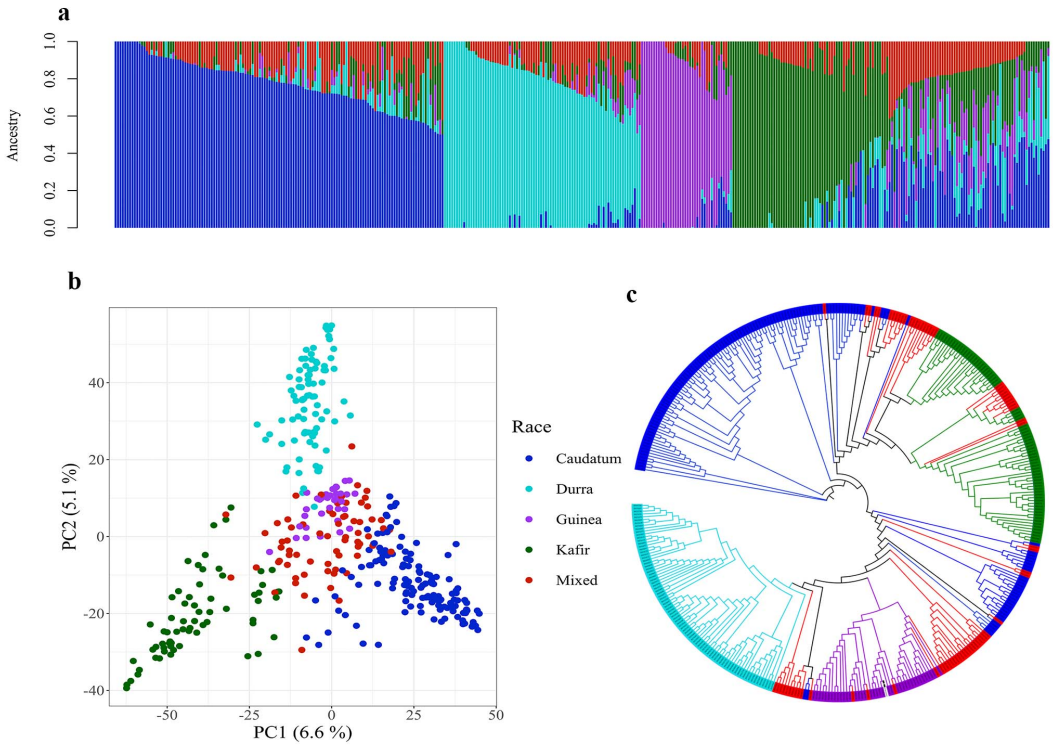

Figure 2. Population structure and clustering analysis of the sorghum diversity panel based on; a) ancestry coefficients for K=5 in admixture, b) principal component analysis of the first two PCs, and c) neighbor joining tree analysis. In parentheses, proportion of variation explained by the corresponding PC. Branches and labels in the tree and accessions in PCA are color coded by the race identified from population structure analysis using admixture. Branch represented by broken line in the guinea clade is wild sorghum *S. propinquum*.

Genetic diversity and linkage disequilibrium

Tajima's D and heterozygosity estimates suggest presence of strong genetic bottlenecks in our panel possibly from domestication, adaptation and artificial selection. The average distance over which LD decayed to half of its maximum value was ~20 kb in our panel, which is consistent with previous observations (Hamblin, et al., 2004, Mace, et al., 2013). Whereas, the average distance for LD decay to reach background levels ($r^2 < 0.1$) was around 100 kb, similar to

370 previous observations of Morris, et al. (2013) in global diversity panels. We observed variability
371 in the level of genetic diversity and LD among sorghum races (Table 1). Average expected
372 heterozygosity for all races were significantly different (p-value < 0.01) from each other. The
373 presence of extensive LD, lower genetic diversity and Tajima's D values within kafir suggests
374 the presence of a stronger genetic bottleneck within this race compared to others (Table 1).
375 Among the five racial types, the mixed race had highest average nucleotide diversity (3.5×10^{-5})
376 and lowest LD. The race guinea had the highest average expected heterozygosity (0.5), whereas
377 the average distance to LD decay for guinea were higher than all races except kafir. Genetic
378 diversity and LD for durra were similar to that of the whole panel. Although LD and nucleotide
379 diversity estimates of caudatum were comparable to that of guinea, heterozygosity in caudatum
380 was about 30% of guinea (Table 1). We calculated the Euclidean distance between the centroids
381 of five PCs and also estimated F_{st} for different races and found that kafir and mixed were
382 genetically the most and least distant race, respectively, whereas the other three races (caudatum,
383 durra, and guinea) seemed to be roughly equidistant from each other (Supplementary Table S1).
384 These results show consistency with the timeline of diversification of these races, as kafir is the
385 most recent and mixed race has some of the most primitive accessions of intermediate and
386 bicolor race.

387 **Table 1**. Summary statistics of whole genome estimates for genetic diversity and LD.

	Whole panel	Mixed	Kafir	Durra	Caudatum	Guinea
Number of accessions	389	67	65	82	137	38
Average heterozygosity[a]	0.17	0.19	0.12	0.18	0.14	0.5
Nucleotide diversity (10^{-5})	3.23	3.48	2.32	3.07	3.01	3.12
Tajima's D	-0.63	-0.93	-1.2	-0.88	-1.01	-0.92
Average r^2	0.09	0.1	0.21	0.1	0.11	0.16
LD decay distance (bp)	20491	14625	145252	19870	32076	39712

388 [a]Nei's unbiased estimator of gene diversity (Nei, 1987)

Phenotypic variation and correlation

The differences between the population means of at least some of the races were significantly different (p-value < 10^{-5}) for all traits except FLH and PH. Phenotypic mean and standard deviation for individual races are listed in Supplementary Table S2. Variation in phenotypic distribution and correlation between traits was observed across all traits (Figure 3). Grain yield was positively correlated with both GN and GW while the two yield components (GN and GW) were slightly negatively correlated to each other. While BL showed a significantly negative correlation with grain yield traits, remaining plant and inflorescence architecture traits (PH, FLH and PL) didn't exhibit any significant correlation to grain yield traits. Grain yield, GN, PH, FLH were all significantly positively correlated with DTA, whereas PL and GW showed significantly negative correlation with DTA.

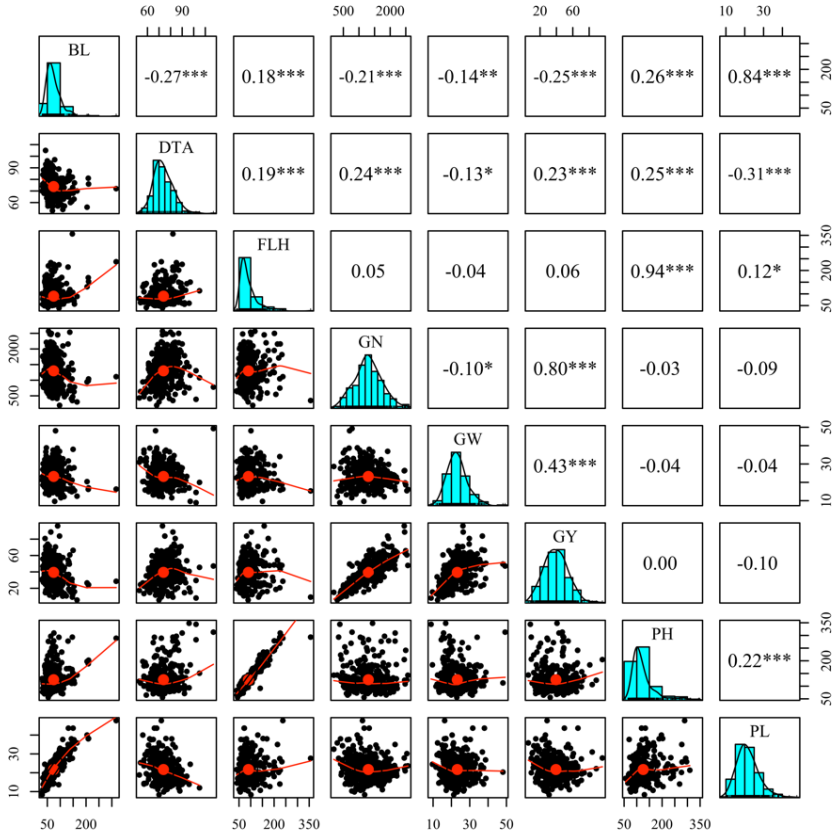

401 **Figure 3**. Distribution and pairwise correlations for adjusted phenotypic mean for all eight traits.
402 Histograms for traits is displayed along the diagonal. Scatterplots with line of fit (red line) for all
403 individuals in the diversity panel are to the left and below the diagonal. Pearson correlation
404 coefficient between the traits shown above the diagonal and to the right. Significance level: *p <
405 0.05, **p < 0.01, **p < 0.001. BL: panicle branch length, DTA: days to anthesis, FLH: flag leaf
406 height, GN: grain number per primary panicle, GW: thousand grain weight, GY: grain yield per
407 primary panicle, PH: plant height, PL: panicle length.

408 **Prediction accuracy and racial structure**

409 The total genomic heritabilities of the traits were strongly correlated (0.63) with *r* from CV1
410 method. For the CV1 method, the highest and lowest *r* were 0.69 for GW and 0.52 for GN and
411 DTA, respectively. Among the traits studied, PH and GN had the highest and lowest genomic
412 heritabilities, respectively (Figure 4a). Despite low heritability, GY had a mean *r* of 0.57 for the
413 CV1 method and DTA had lowest *r* (0.52) despite moderate-high genomic heritability (0.73). As
414 expected, *r* from the CV1 method were always higher than *r* from CV2 prediction methods for
415 all traits, which can be ascribed to the larger training population size and similar population
416 structure between training and validation population in CV1 (Table 2).

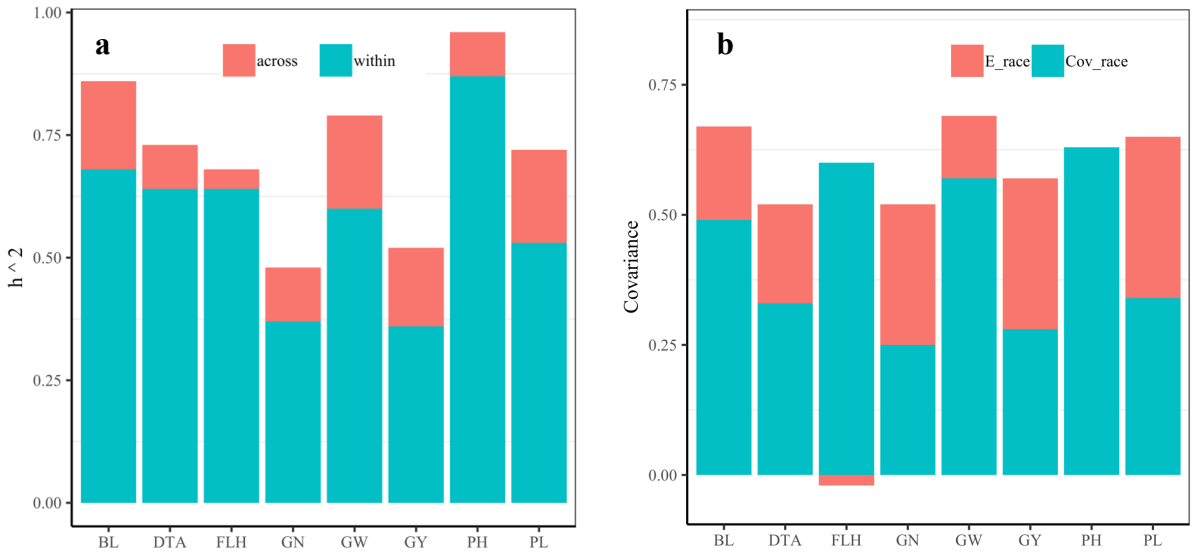

Figure 4. Posterior means of, **a**) within-subpopulation and across-subpopulation genomic heritabilities using first five principal components, **b**) scaled covariances due to condition expectation of race in CV1 prediction. *E_race* represents covariance due to race, and *Cov_race* represents covariance due to individuals within race. h^2, genomic heritability; PH, plant height; GW, thousand grain weight; FLH, flag leaf height; GN, grain number per panicle; GY, grain yield per primary panicle; DTA, days to anthesis; BL, primary branch length; PL, panicle length.

Table 2. Genomic heritability (h^2) and mean prediction accuracy (*r*) of different cross validation methods for all traits studied. Values represent mean ± standard deviation. CV1: cross validation method-1, AR: across race, WR: within race, SRT: single race training.

Trait	CV1	WR	AR	SRT
Days to anthesis (DTA)	0.52 ± 0.01	0.24 ± 0.23	0.12 ± 0.32	0.11 ± 0.23
Flag leaf height (FLH)	0.58 ± 0.03	0.41 ± 0.23	0.34 ± 0.33	0.32 ± 0.21
Grain number/panicle (GN)	0.52 ± 0.02	0.25 ± 0.12	0.27 ± 0.30	0.26 ± 0.20
1000-grain weight (GW)	0.69 ± 0.02	0.61 ± 0.10	0.37 ± 0.27	0.43 ± 0.20
Grain yield/panicle (GY)	0.57 ± 0.02	0.36 ± 0.12	0.35 ± 0.30	0.38 ± 0.17
Plant height (PH)	0.63 ± 0.02	0.46 ± 0.15	0.45 ± 0.28	0.36 ± 0.18
Panicle length (PL)	0.65 ± 0.01	0.25 ± 0.31	0.12 ± 0.33	0.14 ± 0.21
Terminal branch length (BL)	0.67 ± 0.07	0.38 ± 0.24	0.20 ± 0.31	0.26 ± 0.19

428 Figure 4b shows decomposition of the CV1 accuracy into covariances resulting from
429 conditional expectation of races. The scaled covariances E_{race} and Cov_{race} represent expectation
430 due to race and covariances due to individuals within race, respectively. The mean covariances
431 E_{race} and Cov_{race} were positively correlated with posterior means of across (0.61) and within race
432 (0.81) genomic heritabilities, respectively. The estimates for covariances E_{race} and Cov_{race} were
433 comparable to estimates of *r* for AR and WR prediction, respectively, except for height. The
434 estimates of covariances and variance of predicted values for AR prediction method were smaller
435 than in WR (Supplementary Table S3). Hence, the differences in mean *r* between the two
436 methods weren't as pronounced as seen in rice and maize (Guo, et al., 2014).
437 Among CV2 prediction methods, estimates of *r* for WR were higher than AR for BL,
438 DTA, FLH, GW and PL, but the two methods had similar estimates for PH, GN and GY (Table
439 2). However, *r* for different CV2 methods varied depending on the combination of trait and race
440 (Supplementary Table S4). Posterior means of within-subpopulation genomic heritabilities were
441 moderately correlated (0.4) to mean *r* from WR prediction. The average *r* for WR were higher
442 than AR for caudatum and durra whereas the two methods had similar average for guinea, kafir,
443 and mixed (Supplementary Table S4). Plant height and FLH showed smaller difference in *r*
444 between AR and WR prediction across all races, whereas GW showed consistently higher
445 estimates of *r* for WR over AR for all races. Among all the traits, GW had highest mean *r* for
446 WR (0.61) and SRT (0.43) prediction methods, while PH (0.45) had highest *r* for AR.
447 In SRT method, the traits that are heavily correlated to racial structure (DTA, PL, BL,
448 GN and GY) were poorly predicted than PH, FLH and GW (Figure 5). In general, the races durra
449 and caudatum resulted in poor prediction for SRT method when introduced in model as training
450 or validation populations compared to mixed and guinea races (Figure 5). While mixed race is

more closely related to all other races, consistently better performance of guinea and kafir as validation population could be due the amount of shared (versus population-specific) allelic variation in these groups. We observed higher proportions of intermediate frequency minor alleles (0.1 to 0.4) in mixed and guinea than in caudatum, durra and kafir (Supplementary Figure S3). We identified private alleles in each races as the minor alleles that were present in a particular race and were absent in all other races. Within the mixed race group, there were 3,378 private polymorphisms that were not present in any of the other races, although on average these were only present at low frequencies within the population mean (MAF = 0.03). Caudatum had fewer private polymorphisms (1,843), with a mean MAF of 0.04. Durra, on the other hand, had the highest number of private SNPs with 3,969 and the highest MAF for these sites (0.07). Whereas the races kafir and guinea had no private alleles.

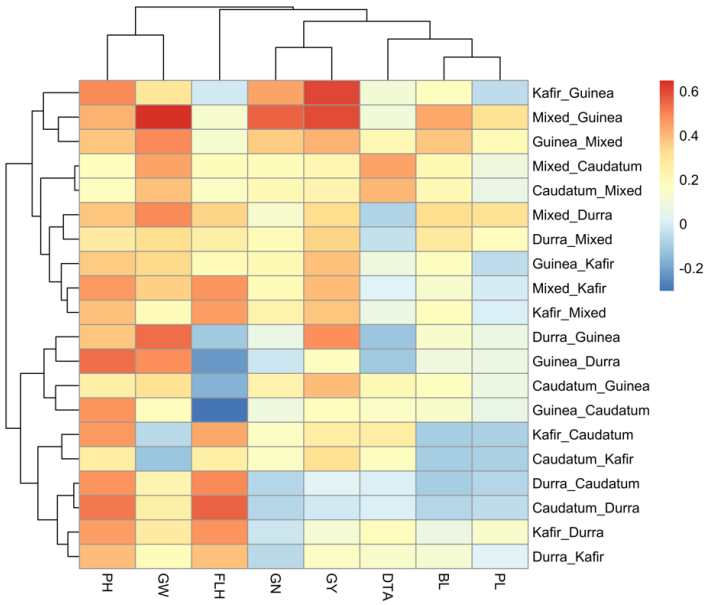

Figure 5. Heatmap showing mean prediction accuracies (*r*) from pairwise single race (SRT) prediction in CV2 prediction method. The races to the right of the heatmap represent training race followed by validation race. Tree cluster to the top and left is based on hierarchical clustering of the values from column and rows, respectively. PH, plant height; GW, thousand

grain weight; FLH, flag leaf height; GN, grain number per panicle; GY, grain yield per primary panicle; DTA, days to anthesis; BL, primary branch length; PL, panicle length.

In order to assess the effect of training population size in *r* for AR and WR method, we ran cross validations using accessions in race caudatum using training population sizes of 28, 52, 74, 96, and 110. Cross-validations were only done for PH, GN, GW, and GY as they represent adequate contrast for trait genetic architecture. While increasing training population size showed consistent increase in *r* for WR prediction of all four traits, increasing training population size did not always lead to increased *r* in AR prediction (Figure 6). Mean *r* for WR was always higher than AR for GW across all training population sizes, whereas they were similar for PH among the two methods. For GN and GY, *r* was higher for AR prediction when training population size was 28 individuals and similar when training population size was 52. At larger training population size, WR prediction method had larger *r* than AR prediction.

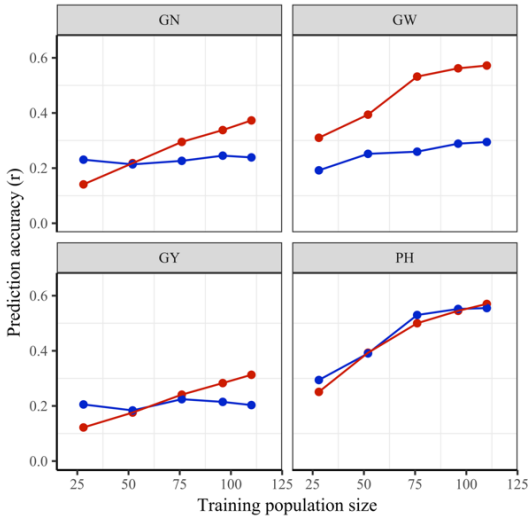

Figure 6. Mean prediction accuracies from across race (AR) and within race (WR) prediction methods for different training population sizes in caudatum. Colors represent cross validation methods, blue = AR, red = WR. GN = grain number, GW = grain weight, GY = grain yield, PH = plant height.

484 **DISCUSSION**

485 **Genetic differentiation and racial structure**

486 The results from the population structure analysis support five subpopulation clusters in our
487 sorghum diversity panel. While the four subpopulations were congruent with the four most
488 recent sorghum races, the bicolor race was not diverged enough to form one distinct group. This
489 is consistent with previous observations from clustering analysis in populations consisting of
490 diverse sorghum accessions (Brown, et al., 2011, Deu, et al., 2006, Wang, et al., 2013). The
491 hypothesis of Harlan and Stemler (1976) that the guinea race was probably the earliest to have
492 diverged from the early bicolor domesticates is supported by our neighbor joining analysis
493 (Figure 2c). *Sorghum propinquum*, an outgroup diploid species from southeast Asia, clustering
494 together with the guinea clade suggests guinea potentially diverged from the early bicolor prior
495 to the divergence of kafir, durra and caudatum. Furthermore, we also see a large proportion of
496 shared alleles and higher allelic diversity among guinea than the evolutionarily recent races,
497 which, however, could also be due to higher rate of gene flow.

498 **Genetic diversity and linkage disequilibrium**

499 Our diversity panel is representative of much of the genetic, phenotypic and geographic diversity
500 of the global sorghum germplasm, and therefore it is an excellent resource for genetic dissection
501 of agronomically important traits and adaptation. Patterns of LD, Tajima's D and genetic
502 diversity from the whole population and within different races suggest strong genetic bottlenecks
503 in our population as a result of domestication, adaptation, and artificial selection. The rate of LD
504 decay, Tajima's D and genetic diversity in our population were comparable to estimates from
505 previous studies (Hamblin, et al., 2004, Mace, et al., 2013, Wang, et al., 2013). Average distance
506 to half decay of LD was similar to that reported by Mace, et al. (2013) for improved inbreds, and

507 lower than the previous estimates of Morris, et al. (2013). Wang, et al. (2013) using 242 diverse
508 accessions from a sorghum mini core collection and 13,390 SNPs, found that LD decayed to
509 background levels between 10 and 30 kb for all but chromosome 2. Average r^2 for different
510 sorghum races in our study were consistent with estimates of Wang et al. (2013). Genetically
511 least diverse racial types (kafir and caudatum) showed higher extents of LD than the races with
512 higher diversity, with the exception of guinea. Previous studies involving separate diversity
513 panels have also reported reduced diversity in kafir (Deu et al. 2006; Casa et al. 2008). The
514 extensive LD and lower heterozygosity in kafir and caudatum might be the result of limited
515 cross-pollination and geographical isolation, whereas genetic drift and smaller sample size could
516 have contributed to slower rate of LD decay in guinea. Bouchet, et al. (2012) also observed
517 similar outcomes for LD and genetic diversity among sorghum races. The lower abundance of
518 private alleles among races kafir and guinea than caudatum and durra was observed by Bouchet,
519 et al. (2012), which is consistent with lack of private alleles for guinea and kafir in our
520 population. Despite being the oldest and most heterozygous race guinea didn't possess any
521 private allele, which could be a result of small sample size of guinea in our population.

522 **Genomic prediction and racial structure**

523 Heritabilities and CV1 prediction accuracy for grain yield and plant height in our study were
524 similar to previous studies in sorghum (Fernandes, et al., 2018, Hunt, et al., 2018, Yu, et al.,
525 2016). Similar heritabilities and *r* for flowering time, panicle length, plant height and grain
526 number have previously been reported in a rice diversity panel (Guo, et al., 2014) . The
527 overwhelming contribution of within-subpopulation genomic heritabilities towards the total
528 genomic heritabilities of traits is comparable to previous observation in rice (Guo, et al., 2014).
529 Grain yield was predicted with consistently higher accuracy than grain number across all cross

530 validation methods despite similar heritabilities of the two traits. While both GN and GY are
531 highly correlated complex traits controlled by a large number of small effect loci, higher
532 accuracy of GY over GN could have resulted from strong positive correlation (0.43) of GY to
533 GW, which has the highest *r*. Traits controlled by large number of small effect loci are predicted
534 with higher accuracy when higher allelic diversity exists in the training population as compared
535 to traits governed by few relatively large effect loci (Norman, et al., 2018). With smaller training
536 sizes for GN and GY the breadth of genetic diversity from all races might have led to boost in *r*
537 for AR over WR, but as training size increased the genomic relatedness in WR appeared to
538 outweigh the effect of genetic diversity, which resulted in stronger positive relationship between
539 *r* and training size in WR (Figure 6). Since the range of training size in our study is small,
540 genetic diversity did not increase substantially with increasing training size resulting in lack of
541 linear relationship between training size and *r* in AR for GN and GY.

542 Population structure resulting from domestication and diversifying selection leads to
543 varying levels of genetic relatedness among individuals within and between subpopulations. The
544 accuracy with which breeding values are estimated is affected by stratification in the population,
545 and the effects are more pronounced when the genetic architecture of the predicted trait is
546 directly associated with population structure (Isidro, et al., 2015, Windhausen, et al., 2012).
547 Previous studies have shown that when population structure in training and testing populations is
548 similar, it can contribute positively towards prediction accuracy (Bastiaansen, et al., 2012,
549 Crossa, et al., 2014, Guo, et al., 2014). But when cross validation strategies that constrained
550 population structure were implemented, it resulted in decline of *r* due to the weakened genetic
551 relationship among individuals in training and testing population (Guo, et al., 2014, Ly, et al.,
552 2013, Lyra, et al., 2018, Norman, et al., 2018).

553 In order to understand the contribution of racial structure in prediction accuracy of
554 stratified sampling method, we decomposed the CV1 accuracy into expectation over races (E_{race})
555 and covariance due to individuals within race (Cov_{race}). Almost non-existent E_{race} covariances for
556 the two height traits, FLH and PH, indicates race as predictor either contributed poorly towards
557 prediction of height. On the other hand, race contributed relatively larger proportion of total
558 covariance for grain yield components and panicle architecture traits. Since the racial structure of
559 sorghum can be directly associated with panicle architecture and indirectly to the grain yield
560 components, proportion of across race genomic heritability and covariance due to race were
561 higher for those traits. We saw sharper decline in *r* for AR prediction compared to WR,
562 especially for panicle architecture traits, which could be attributed to poor genomic relationship
563 between training and validation population. Height traits, PH and FLH, that are less associated
564 with racial structure showed smaller decline in *r* than panicle architecture and grain yield traits.
565 The SRT prediction method also showed smaller *r* for pairwise prediction results for the panicle
566 architecture traits than other traits. Yu, et al. (2016) have previously observed that race as a
567 predictor explains higher variation in predicted values of biomass traits than actual phenotypic
568 values in sorghum, suggesting that under the presence of similar racial structure in training and
569 validation population the accuracy of genomic prediction might have been inflated as a result of
570 overemphasis on racial differences (Brown, 2016). Our approach of decomposition of
571 covariances into conditional expectations due to race could be utilized in dissection of impact of
572 population structure in cross validation accuracy from stratified and random sampling methods in
573 diverse as well as breeding populations.
574 Cross validation approaches similar to the one employed in this study have resulted in
575 higher *r* for within population prediction than across population prediction in wheat (Norman, et

al., 2018), rice and maize (Guo, et al., 2014). Although average *r* across all races in our study was higher for within population for most of the traits, the variation in *r* for individual race and trait combination shows interaction between population structure and trait genetic architecture. Higher *r* for WR over AR among the races caudatum and durra could be because of higher proportion of private alleles and smaller proportion of intermediate frequency minor alleles. This could be the reason for smaller difference between average *r* for AR and WR among guinea, kafir and mixed, as these races show lack of private alleles and/or higher genetic diversity. Furthermore, the results from clustering analysis have shown that the mixed race has closest genetic relationship to the rest of the four races. Our SRT prediction which was a good measure of pairwise predictive relationship between two races also shows that kafir, guinea and mixed have better predictive relationship to each other than to caudatum and durra.

Potential applications for sorghum breeding

Genomic prediction was first introduced roughly two decades ago and has been applied in plant breeding for over a decade (Bernardo and Yu, 2007, Meuwissen, et al., 2001). However, studies investigating prospects and applications of genomic prediction in sorghum are limited. A few studies have been reported for biomass traits in diversity panels (Yu et al. 2016; Fernandes et al. 2017), grain yield in pedigreed male inbred lines (Hunt et al. 2018), and a simulation study investigating prospects in a small sorghum breeding program (Muleta et al. 2019). While clearly defined heterotic pools do not exist in sorghum as they do in maize, races have long been exploited by sorghum breeding programs for hybrid production. If we are to exploit the vast genetic diversity of races in sorghum breeding, we need a more comprehensive understanding of how racial structure impacts prediction accuracy for economically and agronomically important traits.

599 Our study suggests maintaining a genetically diverse training population that includes a
600 mixed/intermediate race might boost prediction accuracy when training population size is
601 constrained. This strategy might be beneficial for young and small breeding programs where
602 breeders have limited resource to construct individual training population for different breeding
603 populations (Muleta, et al., 2019). Furthermore, new phenotypic data from diverse lines when
604 added into the training population can allow for maintenance and increase in frequency of
605 advantageous minor alleles in the gene pool. Guinea had the highest mean prediction accuracy
606 for grain yield and grain weight irrespective of prediction method, suggesting a genetically
607 diverse training population is likely to predict the yield potential of best performing guinea more
608 accurately than individuals from any other race. So breeding programs in West Africa, where
609 guinea sorghum is widely grown, could utilize genotypic and phenotypic data from all racial
610 types in training population design for genomic prediction of guinea varieties. Our results from
611 the SRT method showed that moderate prediction accuracy can be gained even by using a single
612 completely unrelated race as a training population for grain yield components and height.
613 Historically, sorghum breeding programs in the US have heavily relied on kafir and caudatum
614 types while genetic diversity from other races are underutilized. While breeding programs with
615 plentiful resources could gain higher selection accuracy by simply increasing training population
616 size and designing several independent training populations, the utilization of interracial
617 diversity in genomic prediction could help in introducing novel sources of variation for diseases
618 and pest resistance as well as genetic variation for increasing yield potential in the long run.
619 Similarly, another way to increase selection accuracy and genetic gain of complex traits is
620 through utilization of trait-assisted and indirect genomic selection when highly heritable and
621 correlated secondary traits are available (Fernandes et al. 2017). For example, durra accessions in

our results show a within race prediction accuracy of 0.33 and 0.43 for grain number and grain yield but an accuracy of 0.81 and 0.79 for branch length and panicle length, respectively. Panicle architecture could be used in indirect or trait-assisted genomic prediction for grain yield by breeding programs dominated by durra type sorghum varieties. In addition to utilization of within and across group genetic variances, optimization algorithms could also help in efficient design of training population for diversity panels and breeding populations (Akdemir, et al., 2015, Isidro, et al., 2015).

For effective use of crop diversity in sorghum breeding, a breeder might want to work with best representatives from all races rather than opting for the best lines of some races (Brown, 2016). In practical applications, prediction accuracy of traits that are affected by population structure can be increased by using genetically distant subpopulations as parental lines (Guo, et al., 2014). Our results can be useful in such an effort because understanding how individuals of certain race respond to models trained using unrelated races can provide insights into how overall genetic diversity can be deployed in prediction of different racial types. For example, the prediction results from our SRT method shows guinea or mixed race with 37 individuals predicted GN and GY in kafir with higher accuracy than from using 52 kafir accessions (Figure 3, Supplementary Table S3). This kind of empirical evidences of predictive relationship can help in identifying trait-specific and race-specific training design for genomic prediction highlighting the need for more explorative and empirical case studies in natural and breeding populations.

642 **CONCLUSION**

643 Similar population structure between training and testing population can have positive impact on
644 accuracy of genomic prediction. However, inflation in prediction accuracy could be an outcome
645 of genomic prediction models overemphasizing racial differences. Prediction accuracy among
646 races with higher proportion of allelic diversity and/or shared alleles is boosted by training
647 population with higher genetic diversity despite poor genomic relationship, whereas genomic
648 relationship outweighed genetic diversity among races with limited diversity and/or presence of
649 unique polymorphisms. Therefore, training population design for a historically diverse and
650 structured population in sorghum requires careful consideration of genetic structure of the testing
651 population. While the sorghum association panel (SAP) was not intended for genomic prediction,
652 the breadth of genetic and phenotypic diversity in this panel can allow for its application as
653 training population for estimation of breeding values of diverse gene bank accessions. To that
654 objective, including more guinea and bicolor accessions to the panel would be beneficial because
655 our results show that accessions in these races boosts prediction accuracy as training and testing
656 population.

657 **ACKNOWLEDGEMENTS**

658 We would like to thank the endowment fund for the Robert and Lois Coker Trustees Chair of
659 Genetics, Wade Stackhouse fellowship, and Clemson University's Public Service and
660 Agriculture agency for their support for our research and training. We are grateful to Jianming
661 Yu, Jim Holland and Jean-Luc Jannink for their helpful comments and suggestions.

SUPPLEMENTAL MATERIAL

Supplementary_File1 consists of three supplementary figures and four supplementary tables.

CONFLICT OF INTEREST

The authors declare no conflict of interest.

666 **REFERENCES**

667 Akdemir, D., J.I. Sanchez and J.-L. Jannink. 2015. Optimization of genomic selection training populations with a
668 genetic algorithm. Genet Sel Evol 47: 38.

669 Albrecht, T., V. Wimmer, H.J. Auinger, M. Erbe, C. Knaak, M. Ouzunova, H. Simianer and C.C. Schon. 2011.
670 Genome-based prediction of testcross values in maize. Theor Appl Genet 123: 339-350. doi:10.1007/s00122-011-
671 1587-7.

672 Alexander, D.H., J. Novembre and K. Lange. 2009. Fast model-based estimation of ancestry in unrelated
673 individuals. Genome Res 19: 1655-1664. doi:10.1101/gr.094052.109.

674 Bastiaansen, J.W., A. Coster, M.P. Calus, J.A. van Arendonk and H. Bovenhuis. 2012. Long-term response to
675 genomic selection: effects of estimation method and reference population structure for different genetic
676 architectures. Genet Sel Evol 44: 3. doi:10.1186/1297-9686-44-3.

677 Bates, D., M. Mächler, B. Bolker and S. Walker. 2015. Fitting Linear Mixed-Effects Models Using lme4. Journal of
678 Statistical Software 67: 48. doi:10.18637/jss.v067.i01.

679 Bernardo, R. and J. Yu. 2007. Prospects for genomewide selection for quantitative traits in maize. Crop Science 47:
680 1082-1090.

681 Bouchet, S., D. Pot, M. Deu, J.F. Rami, C. Billot, X. Perrier, R. Rivallan, L. Gardes, L. Xia, P. Wenzl, A. Kilian and
682 J.C. Glaszmann. 2012. Genetic structure, linkage disequilibrium and signature of selection in Sorghum: lessons from
683 physically anchored DArT markers. PLoS One 7: e33470. doi:10.1371/journal.pone.0033470.

684 Boyles, R.E., E.A. Cooper, M.T. Myers, Z. Brenton, B.L. Rauh, G.P. Morris and S. Kresovich. 2016. Genome-Wide
685 Association Studies of Grain Yield Components in Diverse Sorghum Germplasm. Plant Genome 9.
686 doi:10.3835/plantgenome2015.09.0091.

687 Boyles, R.E., B.K. Pfeiffer, E.A. Cooper, B.L. Rauh, K.J. Zielinski, M.T. Myers, Z. Brenton, W.L. Rooney and S.
688 Kresovich. 2017. Genetic dissection of sorghum grain quality traits using diverse and segregating populations. Theor
689 Appl Genet 130: 697-716. doi:10.1007/s00122-016-2844-6.

690 Brown, P.J. 2016. Plant breeding: Effective use of genetic diversity. Nat Plants 2: 16154.
691 doi:10.1038/nplants.2016.154.

692 Brown, P.J., P.E. Klein, E. Bortiri, C.B. Acharya, W.L. Rooney and S. Kresovich. 2006. Inheritance of inflorescence
693 architecture in sorghum. Theor Appl Genet 113: 931-942. doi:10.1007/s00122-006-0352-9.

694 Brown, P.J., S. Myles and S. Kresovich. 2011. Genetic support for phenotype-based racial classification in sorghum.
695 Crop Science 51: 224-230.

696 Casa, A.M., G. Pressoir, P.J. Brown, S.E. Mitchell, W.L. Rooney, M.R. Tuinstra, C.D. Franks and S. Kresovich.
697 2008. Community resources and strategies for association mapping in sorghum. Crop Science 48: 30-40.

698 Crossa, J., P. Perez, J. Hickey, J. Burgueno, L. Ornella, J. Ceron-Rojas, X. Zhang, S. Dreisigacker, R. Babu, Y. Li,
699 D. Bonnett and K. Mathews. 2014. Genomic prediction in CIMMYT maize and wheat breeding programs. Heredity
700 112: 48-60. doi:10.1038/hdy.2013.16.

701 Danecek, P., A. Auton, G. Abecasis, C.A. Albers, E. Banks, M.A. DePristo, R.E. Handsaker, G. Lunter, G.T. Marth,
702 S.T. Sherry, G. McVean and R. Durbin. 2011. The variant call format and VCFtools. Bioinformatics 27: 2156-2158.
703 doi:10.1093/bioinformatics/btr330.

704 De Los Campos, G., D. Gianola, G.J. Rosa, K.A. Weigel and J. Crossa. 2010. Semi-parametric genomic-enabled
705 prediction of genetic values using reproducing kernel Hilbert spaces methods. Genetics Research 92: 295-308.

706 de los Campos, G. and D. Sorensen. 2014. On the genomic analysis of data from structured populations. J Anim
707 Breed Genet 131: 163-164. doi:10.1111/jbg.12091.

708 Deu, M., F. Rattunde and J. Chantereau. 2006. A global view of genetic diversity in cultivated sorghums using a
709 core collection. Genome 49: 168-180. doi:10.1139/g05-092.

710 Endelman, J.B. 2011. Ridge Regression and Other Kernels for Genomic Selection with R Package rrBLUP. Plant
711 Genome 4: 250-255. doi:10.3835/plantgenome2011.08.0024.

712 Endelman, J.B. and J.L. Jannink. 2012. Shrinkage estimation of the realized relationship matrix. G3 2: 1405-1413.
713 doi:10.1534/g3.112.004259.

714 Fernandes, S.B., K.O.G. Dias, D.F. Ferreira and P.J. Brown. 2018. Efficiency of multi-trait, indirect, and trait-
715 assisted genomic selection for improvement of biomass sorghum. Theor Appl Genet 131: 747-755.
716 doi:10.1007/s00122-017-3033-y.

717 Glaubitz, J.C., T.M. Casstevens, F. Lu, J. Harriman, R.J. Elshire, Q. Sun and E.S. Buckler. 2014. TASSEL-GBS: a
718 high capacity genotyping by sequencing analysis pipeline. PLoS One 9: e90346. doi:10.1371/journal.pone.0090346.

719 Guo, Z., D.M. Tucker, C.J. Basten, H. Gandhi, E. Ersoz, B. Guo, Z. Xu, D. Wang and G. Gay. 2014. The impact of
720 population structure on genomic prediction in stratified populations. Theor Appl Genet 127: 749-762.
721 doi:10.1007/s00122-013-2255-x.

722 Gusnanto, A., C.C. Taylor, I. Nafisah, H.M. Wood, P. Rabbitts and S. Berri. 2014. Estimating optimal window size
723 for analysis of low-coverage next-generation sequence data. Bioinformatics 30: 1823-1829.
724 doi:10.1093/bioinformatics/btu123.

725 Hadfield, J.D. 2010. MCMC methods for multi-response generalized linear mixed models: the MCMCglmm R
726 package. Journal of Statistical Software 33: 1-22.

727 Hamblin, M.T., S.E. Mitchell, G.M. White, J. Gallego, R. Kukatla, R.A. Wing, A.H. Paterson and S. Kresovich.
728 2004. Comparative population genetics of the panicoid grasses: sequence polymorphism, linkage disequilibrium and
729 selection in a diverse sample of sorghum bicolor. Genetics 167: 471-483.

730 Harlan, J.R. and J.M.J. de Wet. 1972. A Simplified Classification of Cultivated Sorghum1. Crop Science 12: 172-
731 176. doi:10.2135/cropsci1972.0011183X001200020005x.

732 Harlan, J.R. and A. Stemler. 1976. The races of sorghum in Africa. In: J. R. Harlan, J. M. J. de Wet and A. Stemler,
733 editors, Origins of African plant domestication. Mouton Publishers, Paris. p. 465-478.

Hill, W.G. and B.S. Weir. 1988. Variances and covariances of squared linkage disequilibria in finite populations. Theor Popul Biol 33: 54-78.

Hunt, C.H., F.A. van Eeuwijk, E.S. Mace, B.J. Hayes and D.R. Jordan. 2018. Development of Genomic Prediction in Sorghum. Crop Science 58: 690-700. doi:10.2135/cropsci2017.08.0469.

Isidro, J., J.L. Jannink, D. Akdemir, J. Poland, N. Heslot and M.E. Sorrells. 2015. Training set optimization under population structure in genomic selection. Theor Appl Genet 128: 145-158. doi:10.1007/s00122-014-2418-4.

Janss, L., G. de Los Campos, N. Sheehan and D. Sorensen. 2012. Inferences from genomic models in stratified populations. Genetics 192: 693-704. doi:10.1534/genetics.112.141143.

Letunic, I. and P. Bork. 2016. Interactive tree of life (iTOL) v3: an online tool for the display and annotation of phylogenetic and other trees. Nucleic Acids Res 44: W242-245. doi:10.1093/nar/gkw290.

Ly, D., M. Hamblin, I. Rabbi, G. Melaku, M. Bakare, H.G. Gauch, R. Okechukwu, A.G. Dixon, P. Kulakow and J.-L. Jannink. 2013. Relatedness and genotype × environment interaction affect prediction accuracies in genomic selection: a study in cassava. Crop Science 53: 1312-1325.

Lyra, D.H., Í.S.C. Granato, P.P.P. Morais, F.C. Alves, A.R.M. dos Santos, X. Yu, T. Guo, J. Yu and R. Fritsche-Neto. 2018. Controlling population structure in the genomic prediction of tropical maize hybrids. Molecular Breeding 38: 126. doi:10.1007/s11032-018-0882-2.

Mace, E.S., S. Tai, E.K. Gilding, Y. Li, P.J. Prentis, L. Bian, B.C. Campbell, W. Hu, D.J. Innes, X. Han, A. Cruickshank, C. Dai, C. Frere, H. Zhang, C.H. Hunt, X. Wang, T. Shatte, M. Wang, Z. Su, J. Li, X. Lin, I.D. Godwin, D.R. Jordan and J. Wang. 2013. Whole-genome sequencing reveals untapped genetic potential in Africa's indigenous cereal crop sorghum. Nat Commun 4: 2320. doi:10.1038/ncomms3320.

McCouch, S., G.J. Baute, J. Bradeen, P. Bramel, P.K. Bretting, E. Buckler, J.M. Burke, D. Charest, S. Cloutier, G. Cole, H. Dempewolf, M. Dingkuhn, C. Feuillet, P. Gepts, D. Grattapaglia, L. Guarino, S. Jackson, S. Knapp, P. Langridge, A. Lawton-Rauh, Q. Lijua, C. Lusty, T. Michael, S. Myles, K. Naito, R.L. Nelson, R. Pontarollo, C.M. Richards, L. Rieseberg, J. Ross-Ibarra, S. Rounsley, R.S. Hamilton, U. Schurr, N. Stein, N. Tomooka, E. van der

758 Knaap, D. van Tassel, J. Toll, J. Valls, R.K. Varshney, J. Ward, R. Waugh, P. Wenzl and D. Zamir. 2013.
759 Agriculture: Feeding the future. Nature 499: 23-24. doi:10.1038/499023a.

760 Meuwissen, T.H., B.J. Hayes and M.E. Goddard. 2001. Prediction of total genetic value using genome-wide dense
761 marker maps. Genetics 157: 1819-1829.

762 Morris, G.P., P. Ramu, S.P. Deshpande, C.T. Hash, T. Shah, H.D. Upadhyaya, O. Riera-Lizarazu, P.J. Brown, C.B.
763 Acharya, S.E. Mitchell, J. Harriman, J.C. Glaubitz, E.S. Buckler and S. Kresovich. 2013. Population genomic and
764 genome-wide association studies of agroclimatic traits in sorghum. Proc Natl Acad Sci 110: 453-458.
765 doi:10.1073/pnas.1215985110.

766 Muleta, K.T., G. Pressoir and G.P. Morris. 2019. Optimizing Genomic Selection for a Sorghum Breeding Program
767 in Haiti: A Simulation Study. G3 9: 391-401. doi:10.1534/g3.118.200932.

768 Nei, M. 1987. Molecular evolutionary genetics. Columbia University Press, New York.

769 Norman, A., J. Taylor, J. Edwards and H. Kuchel. 2018. Optimising Genomic Selection in Wheat: Effect of Marker
770 Density, Population Size and Population Structure on Prediction Accuracy. G3 8: 2889-2899.
771 doi:10.1534/g3.118.200311.

772 Paradis, E. 2010. pegas: an R package for population genetics with an integrated-modular approach. Bioinformatics
773 26: 419-420. doi:10.1093/bioinformatics/btp696.

774 Price, A.L., N.A. Zaitlen, D. Reich and N. Patterson. 2010. New approaches to population stratification in genome-
775 wide association studies. Nat Rev Genet 11: 459-463. doi:10.1038/nrg2813.

776 R Development Core Team. 2016. R: A language and environment for statistical computing. R Foundation for
777 Statistical Computing, Vienna, Austria.

778 Remington, D.L., J.M. Thornsberry, Y. Matsuoka, L.M. Wilson, S.R. Whitt, J. Doebley, S. Kresovich, M.M.
779 Goodman and E.S.t. Buckler. 2001. Structure of linkage disequilibrium and phenotypic associations in the maize
780 genome. Proc Natl Acad Sci 98: 11479-11484. doi:10.1073/pnas.201394398.

Revelle, W.R. 2011. psych: Procedures for Psychological, Psychometric, and Personality Research. R package version 1.1-2. Evanston, Illinois.

Sorensen, D. and D. Gianola. 2007. Likelihood, Bayesian, and MCMC methods in quantitative geneticsSpringer Science & Business Media.

Swarts, K., H. Li, J.R. Navarro, D. An, M. Romay, S. Hearne, C. Acharya, J. Glaubitz, S. Mitchell and R. Elshire. 2014. FSFHap (Full-Sib Family Haplotype Imputation) and FILLIN (Fast, Inbred Line Library ImputatioN) optimize genotypic imputation for low-coverage, next-generation sequence data in crop plants. Plant Genome 7: 1-12.

Technow, F., C. Riedelsheimer, T.A. Schrag and A.E. Melchinger. 2012. Genomic prediction of hybrid performance in maize with models incorporating dominance and population specific marker effects. Theor Appl Genet 125: 1181-1194. doi:10.1007/s00122-012-1905-8.

Wang, Y.H., H.D. Upadhyaya, A.M. Burrell, S.M. Sahraeian, R.R. Klein and P.E. Klein. 2013. Genetic structure and linkage disequilibrium in a diverse, representative collection of the C4 model plant, Sorghum bicolor. G3 3: 783-793. doi:10.1534/g3.112.004861.

Wendorf, F., A.E. Close, R. Schild, K. Wasylikowa, R.A. Housley, J.R. Harlan and H. Królik. 1992. Saharan exploitation of plants 8,000 years BP. Nature 359: 721-724. doi:10.1038/359721a0.

Wickham, H. 2016. ggplot2: Elegant Graphics for Data Analysis. Springer-Verlag, New York.

Windhausen, V.S., G.N. Atlin, J.M. Hickey, J. Crossa, J.L. Jannink, M.E. Sorrells, B. Raman, J.E. Cairns, A. Tarekegne, K. Semagn, Y. Beyene, P. Grudloyma, F. Technow, C. Riedelsheimer and A.E. Melchinger. 2012. Effectiveness of genomic prediction of maize hybrid performance in different breeding populations and environments. G3 2: 1427-1436. doi:10.1534/g3.112.003699.

Yu, X., X. Li, T. Guo, C. Zhu, Y. Wu, S.E. Mitchell, K.L. Roozeboom, D. Wang, M.L. Wang, G.A. Pederson, T.T. Tesso, P.S. Schnable, R. Bernardo and J. Yu. 2016. Genomic prediction contributing to a promising global strategy to turbocharge gene banks. Nat Plants 2: 16150. doi:10.1038/nplants.2016.150.

805